

Electronic Supplementary Information (ESI)

Triazatruxene-based small molecules with thermally activated delayed fluorescence, aggregation-induced emission and mechanochromic luminescence properties for solution-processable nondoped OLEDs

Yonghong Chen,^{ab} Shumeng Wang,^a Xiaofu Wu,^a Yuxiang Xu,^{ab} Hua Li,^{ac} Yang Liu,^{ac} Hui Tong^{*ac} and
Lixiang Wang^{*ac}

^a State Key Laboratory of Polymer Physics and Chemistry, Changchun Institute of Applied Chemistry, Chinese Academy of Sciences, Changchun 130022, P. R. China.

E-mail: chemtonghui@ciac.ac.cn, lixiang@ciac.ac.cn.

^b University of Chinese Academy of Sciences, Beijing 100049, P. R. China.

^c University of Science and Technology of China, Hefei 230026, P. R. China.

Table of Contents

- 1. General Information**
- 2. OLED fabrication and characterization**
- 3. Material synthesis and characterization**
- 4. Figures and tables**
- 5. References**

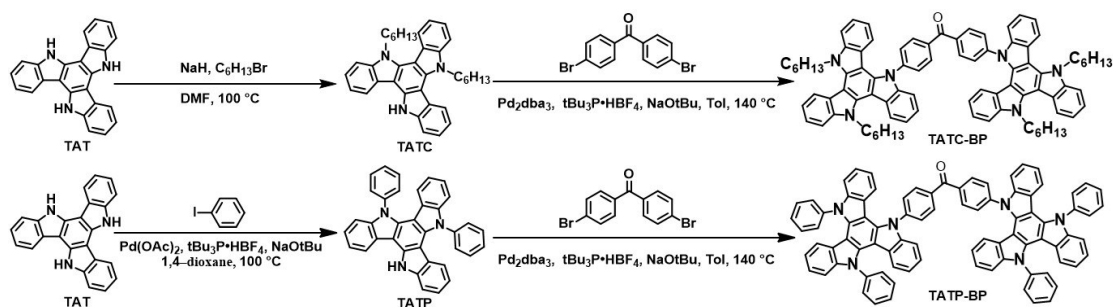
1. General Information

All the starting chemicals for the synthesis were purchased from commercial sources and used as received without purification unless otherwise noted. All the solvents used for the synthesis were dried by sodium or calcium hydride and distilled under argon atmosphere. ^1H -NMR and ^{13}C -NMR spectra were measured with a Bruker Avance NMR spectrometer at room temperature. MALDI-TOF mass spectra were recorded on an AXIMA CFR MS apparatus (COMPACT). Thermal gravimetric analysis (TGA) were measured with a Perkin-Elmer-TGA 7 under nitrogen atmosphere at a heating rate of 20 °C /min. Differential scanning calorimetry (DSC) were measured with Perkin-Elmer-DSC 7 under nitrogen atmosphere at a heating rate of 10 °C /min. UV-vis absorption and photoluminescence spectra were measured with a Perkin-Elmer Lambda 35 UV-vis spectrometer and a Perkin-Elmer LS 50B spectrofluorometer at room temperature, respectively. The photoluminescence quantum yields (PLQYs) were measured with a calibrated integrating sphere system (HORIBA FL-1000). Fluorescence lifetimes were measured using an Edinburgh fluorescence spectrometer (FLS-920). Cyclic voltammetry (CV) curves was recorded on a CHI660a electrochemical analyzer with Bu_4NClO_4 as the electrolyte, a glass carbon electrode as the working electrode, a saturated calomel electrode as the reference electrode and a Pt wire as the counter electrode. The Powder X-ray diffraction patterns (PXRD) measurement was performed using a Bruker D8 Advanced X-ray diffraction ($\lambda = 1.54 \text{ \AA}$).

2. OLED fabrication and characterization

All the devices were fabricated on indium tin oxide (ITO) substrates with a sheet resistance of 15 Ω/sq . The ITO substrates were cleaned with acetone, detergent, distilled water in sequence, and then in an ultrasonic solvent bath. After dried at 120 °C for 2 h, the ITO substrates were treated with UV-ozone for 25 min. PEDOT: PSS (P4083) was spin-coated on the top of the ITO substrate at a speed of 5000 rpm for 40 s, then dried at 120 °C for 45 min. The solutions of the emitters (10 mg/mL in chlorobenzene) were spin-coated on PEDOT:PSS layer as the EML at a speed of 1500 rpm for 60 s. The substrate was transferred to a vacuum deposition chamber, a 55-nm-thick film of TmPyPB, a 1-nm thick film of LiF and 150-nm-thick aluminum were evaporated in sequence through a shadow mask with an array of 14 mm² at a pressure of 4.0×10^{-4} Pa. The EL spectra and CIE coordinates were measured by using a CS2000 spectra colorimeter. The current–voltage and brightness–voltage characteristics of the devices were measured by using a Keithley 2400/2000 source meter with a calibrated silicon photodiode. All the measurements were carried out under ambient conditions at room temperature.

3. Material synthesis and characterization



Scheme S1 Synthetic routes of TATC-BP and TATP-BP.

10,15-dihydro-5H-diindolo[3,2-a:3',2'-c]carbazole (TAT) was synthesized using the previously reported method.^{1, 2}

Synthesis of 5,10-dihexyl-10,15-dihydro-5H-diindolo[3,2-a:3',2'-c]carbazole (TATC).

A mixture of triazatruxene core (TAT) (5.00 g, 14.48 mmol) and NaH (0.76 g, 31.86 mmol) in DMF (100 mL) was stirred for 4 h under argon at room temperature, then bromohexane (5.02 g, 30.41 mmol) was added dropwise, and the reaction mixture was heated up to 100 °C for 24 h. The mixture was diluted with dichloromethane (DCM), washed with water. The organic layer was dried with Na₂SO₄ and the solvent were evaporated under vacuum. The crude product was purified on a silica gel column using DCM/PE: 1/3 as mobile phase to give TATC (2.21 g, 30%) as a grey white solid. ¹H NMR (500 MHz, CDCl₃) δ (ppm) 8.70 (s, 1H), 8.27 (d, J = 8.0 Hz, 2H), 8.06 (s, 1H), 7.63 (d, J = 7.6 Hz, 1H), 7.58 (d, J = 8.2 Hz, 2H), 7.47 (t, J = 7.1 Hz, 2H), 7.41 (t, J = 7.2 Hz, 2H), 7.33 (s, 2H), 4.79 (s, 4H), 2.10 (m, 4H), 1.37 (m, 12H), 0.88 (m, 6H). ¹³C NMR (126 MHz, CDCl₃) δ (ppm) 140.63, 139.76, 137.04, 122.61, 122.52, 121.66, 121.31, 119.89, 119.38, 111.07, 109.72, 102.70, 46.70, 31.55, 31.50, 26.40, 22.53, 13.96. MALDI-TOF MS (m/z): Calcd for C₃₆H₃₉N₃, Exact Mass: 513.31, Found: 513.3 (M⁺).

Synthesis of bis(4-(10,15-dihexyl-10,15-dihydro-5H-diindolo[3,2-a:3',2'-c]carbazol-5-yl)phenyl)methanone (TATC-BP).

A mixture of 5,10-dihexyl-10,15-dihydro-5H-diindolo[3,2-a:3',2'-c]carbazole (TATC). (0.60 g, 1.16 mmol), bis(4-bromophenyl)methanone (0.14 g, 0.42 mmol), tris(dibenzylideneacetone)dipalladium(0) (38.8 mg, 0.04 mmol), tri-tert-butylphosphine tetrafluoroborate (36.8 mg, 0.13 mmol), sodium tert-butoxide (0.61 g, 6.35 mmol) and toluene (15 ml) was heated at 140 °C under argon for 24 h. The mixture was diluted with dichloromethane (DCM), washed with water. The organic layer was dried with Na₂SO₄ and the solvent were evaporated under vacuum. The crude product was purified on a silica gel column using DCM/PE: 2/1 as mobile phase to give TATC-BP (0.35 g, 69%) as a yellow solid. ¹H NMR (500 MHz, CDCl₃) δ (ppm) 8.34 (d, J = 8.1 Hz, 4H), 8.15 (d, J = 8.3 Hz, 4H), 7.76 (d, J = 8.4 Hz, 4H), 7.69 (d, J = 8.1 Hz, 2H), 7.63 (d, J = 9.0 Hz, 2H), 7.51 (m, 4H), 7.40 (m, 6H), 7.22 (s, 2H), 6.78 (t, J = 7.6 Hz, 2H), 6.24 (d, J = 5.8 Hz, 2H), 4.94 (d, J = 48.1 Hz, 8H), 2.05 (m, 8H), 1.31 (m, 24H), 0.85 (m, 12H). ¹³C NMR (126 MHz, CDCl₃) δ 194.75, 144.78, 141.17, 140.91, 136.27, 131.82, 128.15, 123.45, 123.26, 123.17, 122.92, 122.07, 121.76, 121.62, 121.06, 119.79, 119.05, 110.66, 109.80, 104.24, 47.15, 47.00, 31.44, 31.40, 29.96, 29.88, 26.37, 26.32, 22.49, 22.47, 13.93, 13.90. MALDI-TOF MS (m/z): Calcd for C₈₅H₈₄N₆O, Exact Mass: 1204.67, Found: 1204.7 (M⁺).

Synthesis of 5,10-diphenyl-10,15-dihydro-5H-diindolo[3,2-a:3',2'-c]carbazole (TATP).

A mixture of TAT (5.00 g, 14.48 mmol), iodobenzene (4.43 g, 21.72 mmol), palladium(II) acetate (130.0 mg, 0.58 mmol), tri-tert-butylphosphine tetrafluoroborate (504.0 mg, 1.74 mmol), sodium tert-butoxide (4.17 g, 43.44 mmol) and 1,4-dioxane (80 ml) was heated at 100 °C under argon for 18 h. The mixture was diluted with DCM, washed with water. The organic layer was dried with Na₂SO₄ and the solvent were evaporated under vacuum. The crude product was purified on a silica gel column using DCM/PE: 1/5 as mobile phase to give TATP (2.53 g, 35%) as a white solid. ¹H NMR (500 MHz, DMSO) δ (ppm) 11.99 (s, 1H), 8.86 (d, J = 7.7 Hz, 1H), 7.69 (m, 11H), 7.49 (m, 1H), 7.42 (d, J = 6.8 Hz, 1H), 7.40 (d, J = 7.8 Hz, 1H), 7.21 (t, J = 7.5 Hz, 1H), 7.17 (t, J = 8.0 Hz, 1H), 7.13 (d, J = 7.4 Hz, 1H), 6.72 (m, 1H), 6.65 (t, J = 7.6 Hz, 1H), 5.95

(d, $J = 8.1$ Hz, 1H), 5.75 (d, $J = 8.6$ Hz, 1H). ^{13}C NMR (126 MHz, DMSO) δ (ppm) 141.45, 141.11, 140.67, 140.46, 139.82, 137.84, 136.30, 135.13, 130.70, 130.68, 129.41, 129.18, 129.05, 128.99, 124.20, 123.42, 123.31, 122.97, 122.27, 122.16, 122.01, 121.77, 121.28, 120.69, 120.23, 119.17, 111.41, 110.65, 110.08, 103.53, 102.78, 102.36. MALDI-TOF MS (m/z): Calcd for $\text{C}_{36}\text{H}_{23}\text{N}_3$, Exact Mass: 497.19, Found: 497.2 (M^+).

Synthesis of bis(4-(10,15-diphenyl-10,15-dihydro-5H-diindolo[3,2-a:3',2'-c]carbazol-5-yl)phenyl)methanone (TATP-BP).

A mixture of 5,10-diphenyl-10,15-dihydro-5H-diindolo[3,2-a:3',2'-c]carbazole (TATP) (0.58 g, 1.16 mmol), bis(4-bromophenyl)methanone (0.14 g, 0.42 mmol), tris(dibenzylideneacetone)dipalladium(0) (38.8 mg, 0.04 mmol), tri-tert-butylphosphine tetrafluoroborate (36.8 mg, 0.13 mmol), sodium tert-butoxide (0.61 g, 6.35 mmol) and toluene (15 ml) was heated at 140°C under argon for 24 h. The mixture was diluted with dichloromethane (DCM), washed with water. The organic layer was dried with Na_2SO_4 and the solvent were evaporated under vacuum. The crude product was purified on a silica gel column using DCM/PE: 2/1 as mobile phase to give TATP-BP (0.26 g, 53%) as a yellow solid. ^1H NMR (500 MHz, CDCl_3) δ (ppm) 8.19 (d, $J = 8.4$ Hz, 4H), 7.83 (d, $J = 8.4$ Hz, 4H), 7.65 (m, 20H), 7.51 (d, $J = 8.2$ Hz, 2H), 7.34 (t, $J = 7.7$ Hz, 4H), 7.19 (m, 6H), 6.81 (m, 6H), 6.30 (d, $J = 8.1$ Hz, 2H), 6.07 (dd, $J = 8.1$, 4.7 Hz, 4H). ^{13}C NMR (126 MHz, CDCl_3) δ (ppm) 194.69, 144.83, 141.74, 141.63, 141.09, 140.77, 140.69, 137.71, 137.51, 137.08, 136.33, 131.88, 129.97, 129.00, 128.98, 128.35, 123.45, 123.41, 123.31, 123.09, 122.76, 122.61, 122.29, 122.20, 122.11, 120.62, 120.05, 119.80, 110.14, 109.90, 109.67, 104.99, 104.84, 104.32. MALDI-TOF MS (m/z): Calcd for $\text{C}_{85}\text{H}_{52}\text{N}_6\text{O}$, Exact Mass: 1172.42, Found: 1172.4 (M^+).

4. Figure and tables

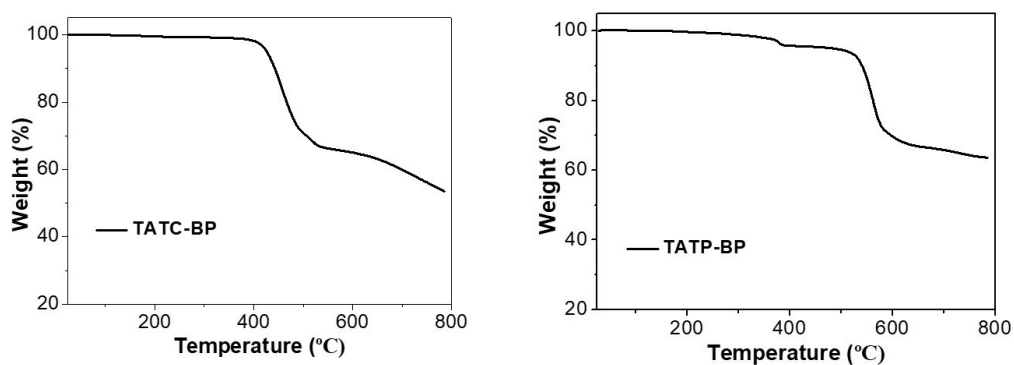


Fig. S1. The thermogravimetric thermograms of (A) TATC-BP and (B) TATP-BP.

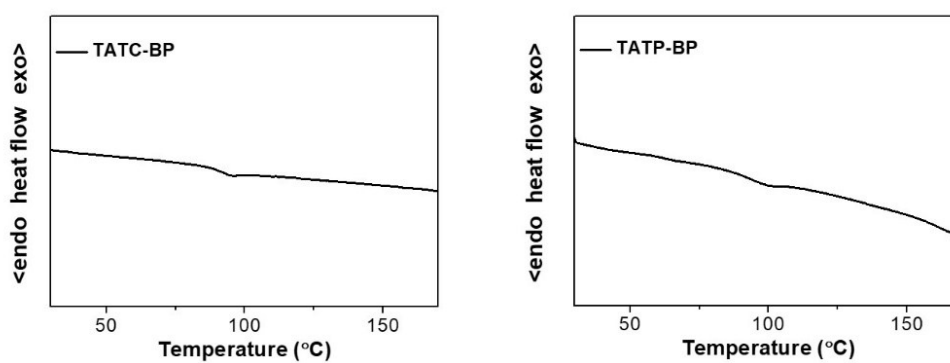


Fig. S2. The differential scanning calorimetry traces of (A) TATC-BP and (B) TATP-BP.

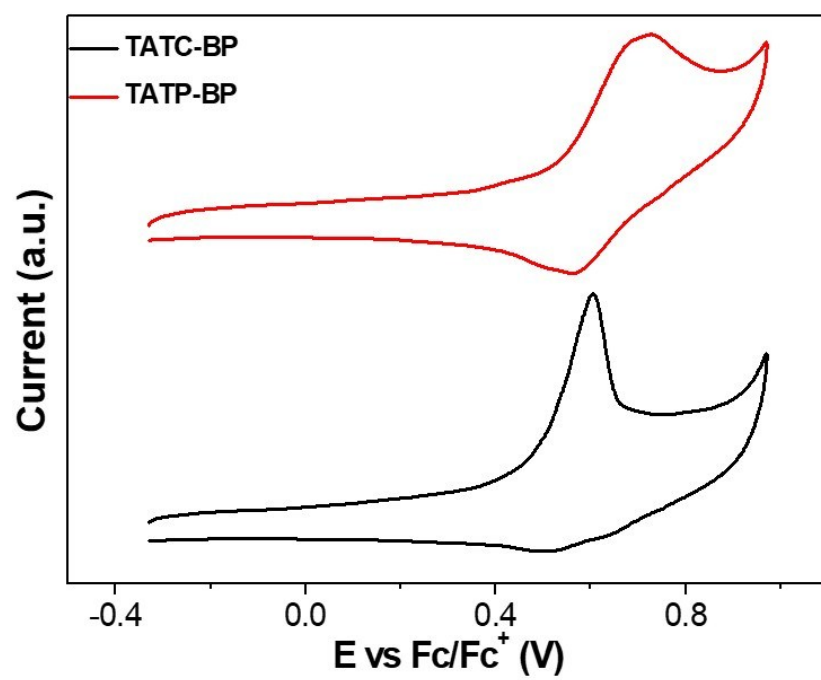


Fig. S3. Cyclic voltammetry analysis of TATC-BP and TATP-BP.

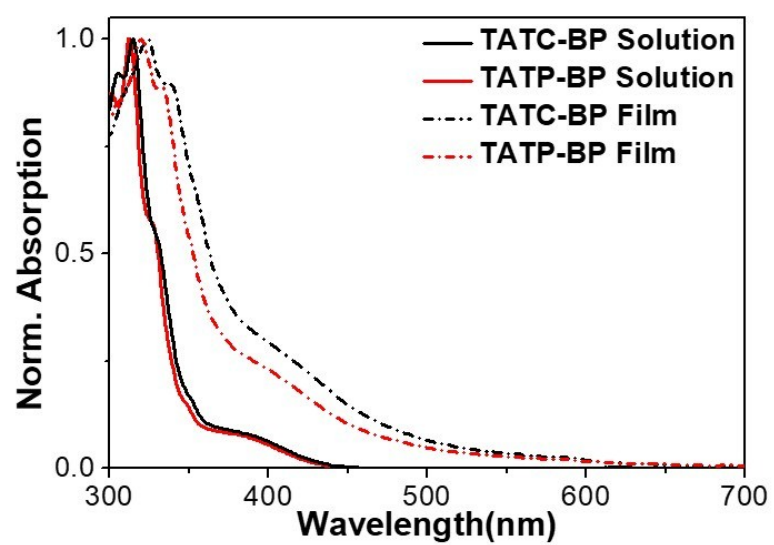


Fig. S4. Absorption spectra in THF solutions and neat films.

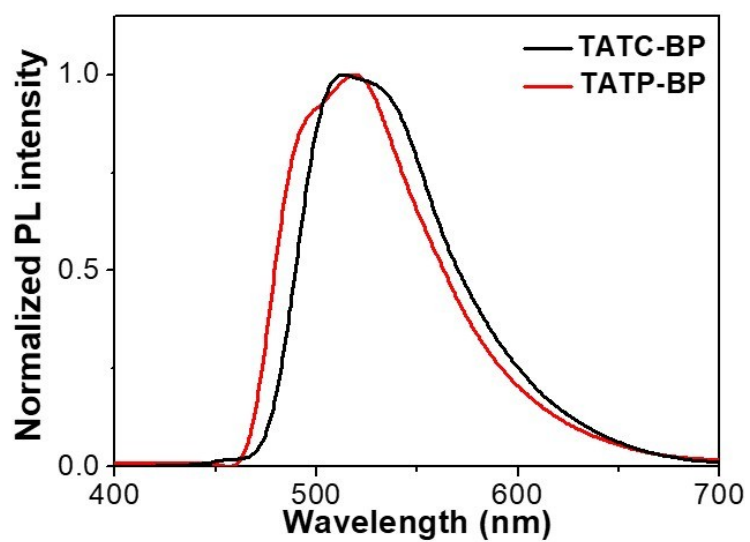


Fig. S5. Phosphorescence spectra of TATC-BP and TATP-BP in neat films.

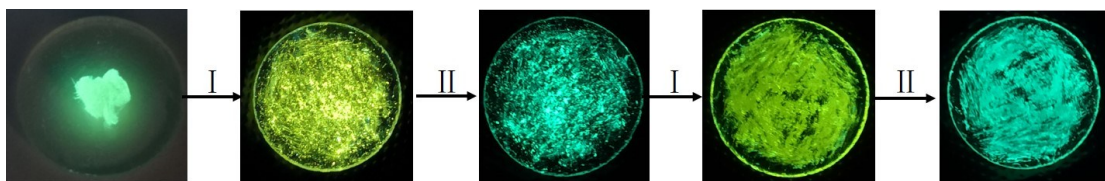


Fig. S6. Repeated switching between blue-green and yellow of the emission of TATC-BP in mortar by grinding and fuming cycles. The images were taken under illumination of a UV lamp. I : after grinding; II : after fuming treatment with dichloromethane.

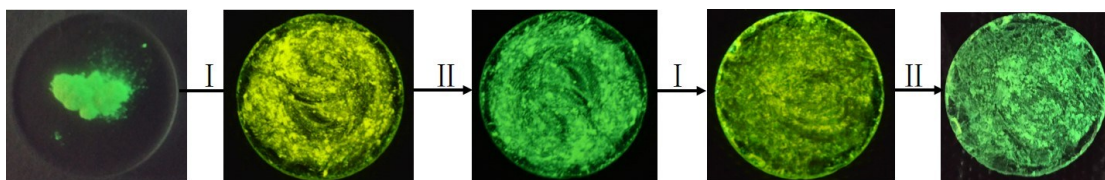


Fig. S7. Repeated switching between green and yellow of the emission of TATP-BP in mortar by grinding and fuming cycles. The images were taken under illumination of a UV lamp. I : after grinding; II : after fuming treatment with dichloromethane.

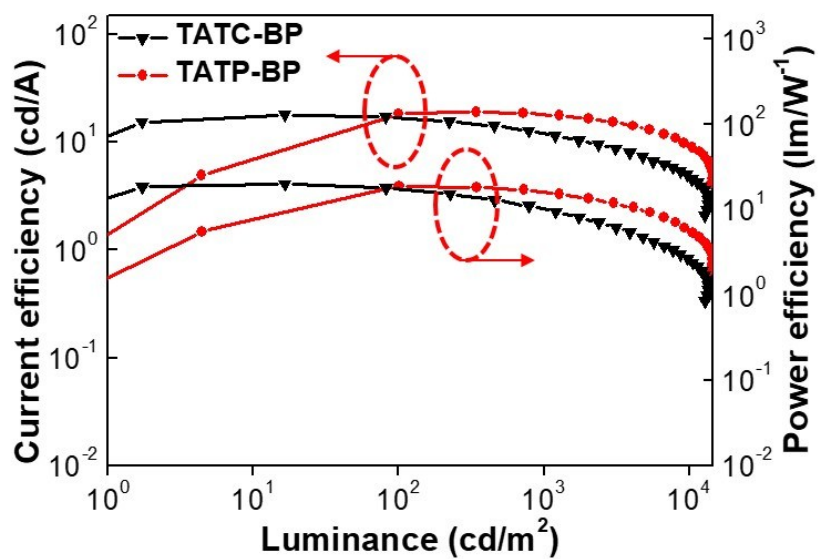


Fig. S8. Current efficiency/luminance/power efficiency curves of the nondoped devices of TATC-BP and TATP-BP.

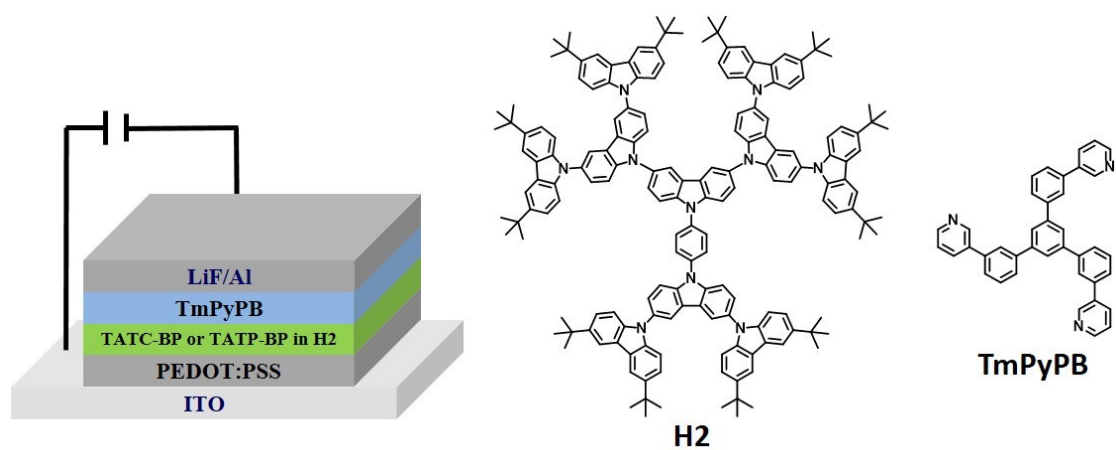


Fig. S9. Doped device configuration and molecular structures of the used materials.

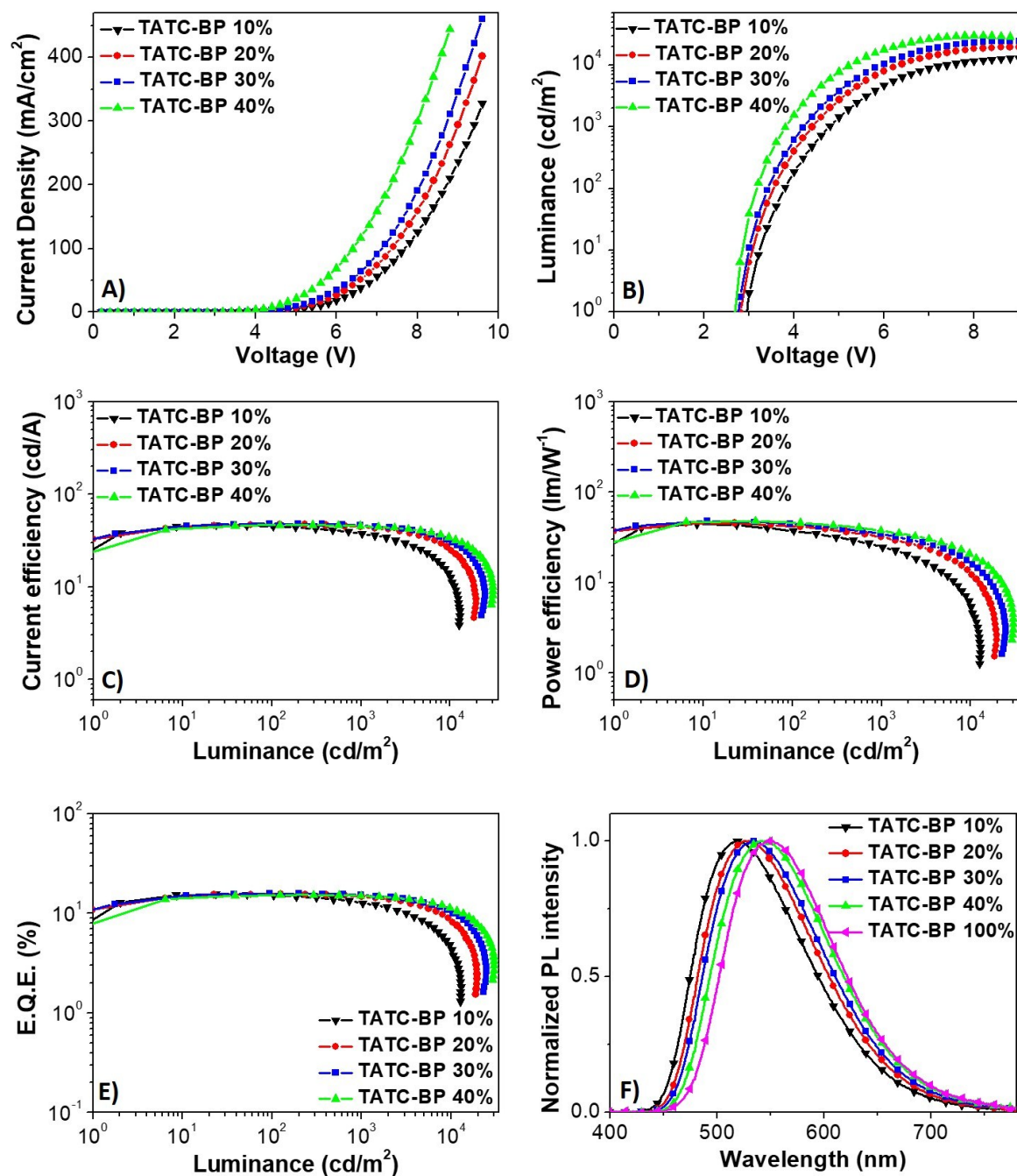


Fig. S10. EL performance of the OLEDs based on TATC-BP doped in H2 host.

A) Current density-voltage characteristics. B) Luminance-voltage characteristics. C) Current efficiency-luminance characteristics. D) Power efficiency-luminance characteristics. E) External quantum efficiency-luminance characteristics. F) EL spectra of the OLED devices at 1000 cd m^{-2} .

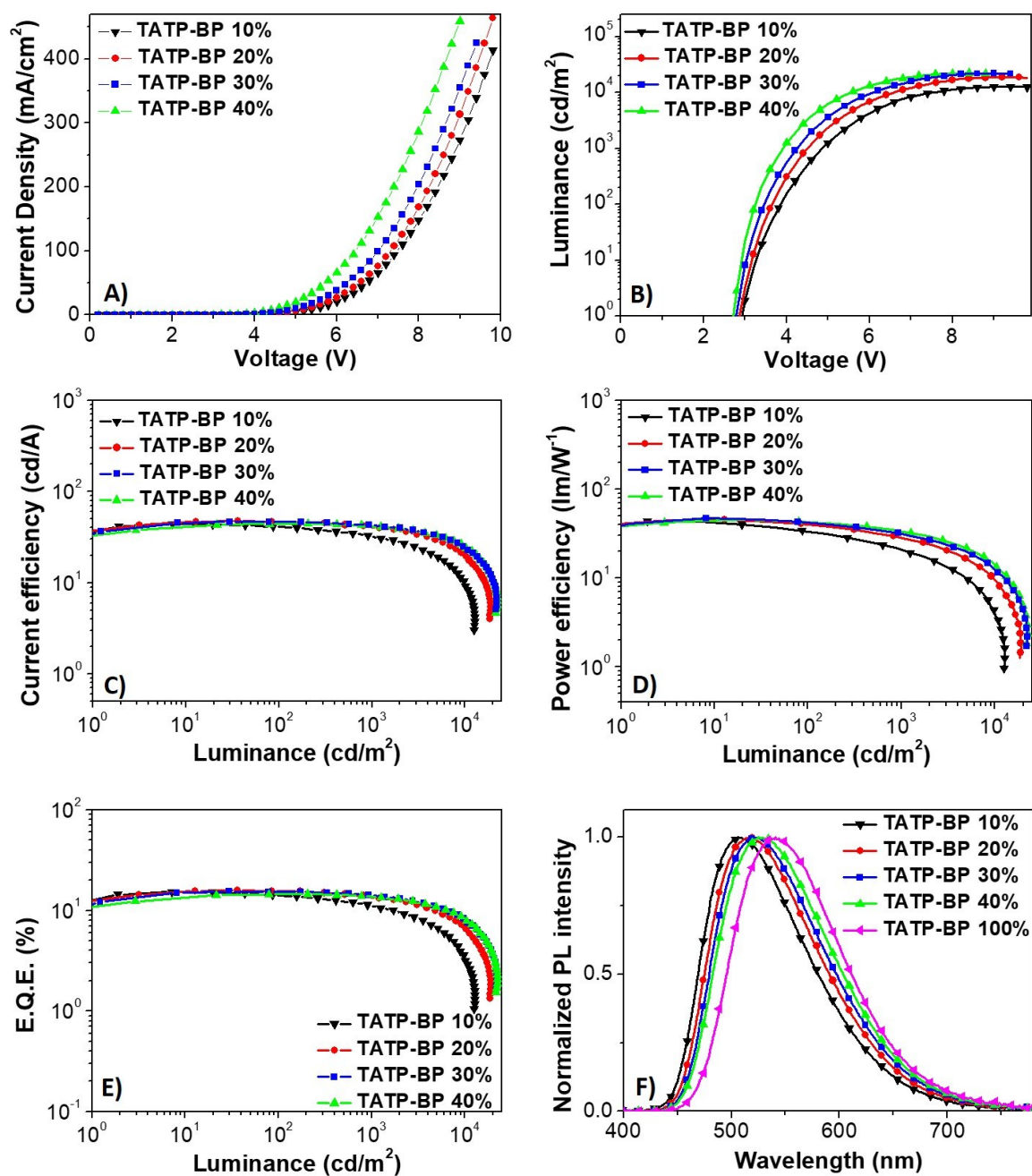


Fig. S11. EL performance of the OLEDs based on TATP-BP doped in H2 host.

A) Current density-voltage characteristics. B) Luminance-voltage characteristics. C) Current efficiency-luminance characteristics. D) Power efficiency-luminance characteristics. E) External quantum efficiency-luminance characteristics. F) EL spectra of the OLED devices at 1000 cd/m^2 .

Table S1. DFT calculation results of TATC-BP and TATP-BP.

Emitters	HOMO	LUMO	S₁	T₁	ΔE_{ST}
	(eV)	(eV)	(eV)	(eV)	(eV)
TATC-BP	-4.85	-1.89	2.55	2.47	0.08
TATP-BP	-4.90	-1.89	2.58	2.48	0.09

Table S2. PLQYs of doped films of TATC-BP and TATP-BP in H2 host with different doping concentration.

Emitters	10%	20%	30%	40%	100%
TATC-BP	50.0%	50.5%	52.7%	46.5%	22.0%
TATP-BP	46.3%	53.9%	55.3%	45.8%	24.2%

Table S3: EL performance of the OLEDs based on TATC-BP doped in H2 with different doping concentration.

Emitters	V _{on} (V)	Max performance			Device performance at 1000 cd m ⁻²				
		LE	PE	EQE	V	LE	PE	EQE	CIE
		(cd/A)	(lm/W)	(%)	(V)	(cd/A)	(lm/W)	(%)	(x,y)
10%	3.0	46.4	44.4	15.7	4.8	37.6	24.6	12.7	0.32, 0.51
20%	2.8	47.5	45.3	15.7	4.4	44.7	31.9	14.8	0.35, 0.53
30%	2.8	48.1	47.8	15.9	4.2	46.3	34.6	15.3	0.37, 0.53
40%	2.7	47.5	47.6	15.4	3.8	45.8	37.8	15.1	0.39, 0.54
100%	2.6	17.8	20.0	5.9	3.7	12.0	10.2	4.8	0.41, 0.54

Table S4: EL performance of the OLEDs based on TATP-BP doped in H2 with different doping concentration.

Emitters	V _{on} (V)	Max performance			Device performance at 1000 cd m ⁻²				
		LE	PE	EQE	V	LE	PE	EQE	CIE
		(cd/A)	(lm/W)	(%)	(V)	(cd/A)	(lm/W)	(%)	(x,y)
10%	2.9	44.0	43.5	15.2	4.8	32.4	20.9	11.2	0.29, 0.49
20%	2.9	47.3	45.8	15.9	4.5	40.8	28.4	13.7	0.32, 0.51
30%	2.8	46.4	47.2	15.4	4.2	42.7	31.6	14.2	0.34, 0.53
40%	2.7	44.4	45.1	14.6	3.9	41.7	33.5	13.7	0.35, 0.53
100%	2.7	18.9	19.2	6.0	3.5	18.0	16.1	5.8	0.38, 0.55

5. Reference

1. F. Wang, X. C. Li, W. Y. Lai, Y. Chen, W. Huang and F. Wudl, *Org. Lett.*, 2014, **16**, 2942-2945.
2. K. Rakstys, A. Abate, M. I. Dar, P. Gao, V. Jankauskas, G. Jacopin, E. Kamarauskas, S. Kazim, S. Ahmad, M. Gratzel and M. K. Nazeeruddin, *J. Am. Chem. Soc.*, 2015, **137**, 16172-16178.